Size Effect on Strength and Lifetime Distributions of Quasibrittle Structures Implied by Interatomic Bond Break Activation

Zdeněk P. Bažant[1a], Jia-Liang Le[1b] and Martin Z. Bazant[2c]

[1]Northwestern University, Evanston, Illinois 60208, USA

[2]Massachusetts Institute of Technology, Cambridge, Massachusetts 02139, USA; and Ecole Supérieure de Physique et de Chimie Industrielles, 75005 Paris, France

[a]z-bazant@northwestern.edu, [b]jialiang-le@northwestern.edu, [c]bazant@math.mit.edu

Keywords: Structural strength, Lifetime; Probabilistic mechanics; Size effect; Scaling; Fracture; Extreme value statistics; Activation energy; Safety factors, Structural reliability.

Abstract. Engineering structures such as aircrafts, bridges, dams, nuclear containments and ships, as well as computer circuits, chips and MEMS, should be designed for failure probability < 10^{-6} to 10^{-7} per lifetime. However, the safety factors required to ensure it are still determined empirically, even though they represent much larger and much more uncertain corrections to deterministic calculations than do the typical errors of modern computer analysis of structures. Bažant and Pang recently developed (and presented at previous ECF) a new theory for the cumulative distribution function (cdf) for the strength of quasibrittle structures failing at macro-fracture initiation, and offered its simplified justification in terms of thermally activated inter-atomic bond breaks. Presented here is a refined justification of this theory based on fracture mechanics of atomic lattice cracks advancing through the lattice by small jumps over numerous activation energy barriers on the surface of the free energy potential of the lattice. For the strength of the representative volume element (RVE) of material, simple statistical models based on chains and bundles are inadequate and a model consisting of a hierarchy of series and parallel couplings is adopted. The theory implies that the strength of one RVE must have a Gaussian cdf, onto which a Weibullian (or power-law) tail is grafted on the left at the failure probability of about 10^{-4} to 10^{-2}. A positive-geometry structure of any size can be statistically modeled as a chain of RVEs. With increasing structure size, the Weibullian part of the cdf of structural strength expands from the left tail and the grafting point moves into the Gaussian core, until eventually, for a structure size exceeding about 10^4 equivalent RVEs, the entire cdf becomes Weibullian. Relative to the standard deviation, this transition nearly doubles the distance from the mean to the point of failure probability 10^{-6}. Contrary to recent empirical models, it is found that the strength threshold must be zero. This finding and the size effect on cdf has a major effect on the required safety factor. The theory is further extended to model the lifetime distribution of quasibrittle structures under constant load (creep rupture). It is shown that, for quasibrittle materials, there exists a strong size effect on not only the structural strength but also the lifetime, and that the latter is stronger. Like the cdf of strength, the cdf of lifetime, too, is found to change from Gaussian with a remote power-law tail for small sizes, to Weibullian for large sizes. Furthermore, the theory provides an atomistic justification for the power-law form of Evans' law for crack growth rate under constant load and of Paris' law for crack growth under cyclic load. For various quasibrittle materials, such as industrial and dental ceramics, concrete and fibrous composites, it is finally demonstrated that the proposed theory correctly predicts the experimentally observed deviations of strength and lifetime histograms from the classical Weibull theory, as well as the deviations of the mean size effect curves from a power law.

Introduction

The safety factors guarding against the uncertainty in structural strength and lifetime are the most uncertain aspect of design. The design of engineering structures such as aircrafts, bridges, dams, nuclear containments, and ships must ensure an extremely low failure probability, generally accepted to be 10^{-6} to 10^{-7}. It is obvious that an experimental verification by strength and lifetime histograms is impossible for such a low probability. Therefore, one must rely on some physically based theory that can be experimentally verified indirectly.

For the cdf of strength of structures (failing at macro-crack initiation), two limiting cases are clearly understood so far: 1) a perfectly ductile failure, for which the strength cdf for any structural size must be Gaussian (except the far-left tail), since the failure load represents essentially a weighted sum of the strength contributions from all the representative volume elements (RVEs) of the material lying on the failure surface; and 2) a perfectly brittle failure, which is decided by the failure at one RVE and consequently must follow the weakest-link model. This model is necessarily Weibullian if the number of RVEs in the structure is very large.

One motivation of this study is the fact that an effect of particular concern for structural reliability and lifetime predictions of quasibrittle structures is the transition from quasi-plastic to brittle response with increasing structure size, and the associated effect of structure type and geometry (or brittleness). Such a transition typically occurs in quasibrittle materials, which include concrete, fiber-polymer composites, tough ceramics, rocks, cohesive stiff soils, sea ice, rigid foams, wood, bone, etc., at normal scale, and many more at the micrometer scale of MEMS and thin films. Extensive strength histograms show that the cumulative distribution function (cdf) of strength for these materials deviates from the two-parameter Weibull cdf, which was thought to imply the Weibull distribution with non-zero threshold. However, for broad-range strength histograms with many thousands of data, a systematic deviation from the experimental histograms still remains.

The strength of large brittle or quasibrittle structures of positive geometry (i.e., failing at crack initiation [5, 6, 13]) depends only on the tail of the strength cdf of a representative volume element (RVE), which was shown to be necessarily a power-law [10, 11, 12], while the distribution core is Gaussian (or normal). A simplified justification of this property was given in terms of thermally activated inter-atomic bond breaks and the stress dependence of the activation energy. The transition from the atomic scale to the RVE scale was statistically described by a model consisting of a hierarchy of elements coupled in parallel and in series [10, 11, 12]. The parallel couplings reflect the fact that a passage from one scale to the next higher scale involves strain compatibility conditions, and the series couplings, in the sense of the weakest-link chain model, reflect damage localization into microcracks.

Although the agreement of this model with the experimental strength histograms and size effect curve of concrete, ceramics and composites was found to be as good as might be desired, the model was found inadequate for extension to the statistics of lifetime at constant load, because of simplifications on the atomic scale. This paper will present a refined probabilistic model which replaces the statistics of severance of atomic bonds by a fracture-mechanics-based statistical analysis of crack propagation through the nano-scale atomic lattice, in order to predict the lifetime distribution. At the same time, this new nano-mechanical approach will provide a more detailed and stronger justification for the statistics of material strength and the size effect (of type 1 [5]).

Recent studies have demonstrated that extensive numerical simulations of crack propagation through an atomic lattice, based on inter-atomic potentials [24] and even direct coupling to quantum mechanics [1, 17], have become feasible, through advances in computational materials science [23, 26]. However, despite the usefulness of such large-scale numerical simulations, there is a great need for a simplified ***analytical*** description that captures the essential behavior in a way showing the main trends and influencing parameters. To fill this need is the goal of this paper.

Thermally Activated Fracture Growth at the Atomic Scale

Let us consider a nano-scale size atomic lattice block undergoing fracture as shown in Fig. 1. At the fracture front, the separation δ between the opposite atoms across the crack gradually increases with decreasing distance x from the crack mouth. The pairs of opposite atoms across the crack are bound with a local potential Π_1 which is a part of the overall potential function Π (or more generally, free energy) of the atomic lattice (crudely, Π_1 could be described as the Morse or Lennard-Jones potential, but a specific form is not needed here).

The equilibrium states of these atomic pairs, or bonds, are marked on the local potential curves $\Pi_1(\delta)$ by the black circles, and the arrows portray thermal fluctuations. As the fracture separation grows wider from one atomic pair to the next, the state marked by the black circle moves on the curve $\Pi_1(\delta)$ up and right. These states are also shown on the curves of bond force $F_b(\delta)$ between the opposite atoms, which represents the slope of curve $\Pi_1(\delta)$. The local bond failure begins when the peak point of the curve $F_b(\delta)$ is reached, and this point corresponds to the point of maximum slope of the curve $\Pi_1(\delta)$ (state 3 in Fig. 1a). This is the point roughly representing the end of the cohesive crack in the lattice. The true crack ends at the pair where the bond force is reduced to 0 (state 5 in Fig. 1a). The fracture process zone (FPZ) in the lattice roughly spans from state 3 to state 5, which are many atoms apart.

As the fracture propagates, the diagram $P(u)$ of load P applied on the lattice block versus the associated displacement u caused by elasticity of lattice and by fracture growth would have the usual shape shown in Fig. 2a if the lattice were treated as a continuum (the rising curved portion would be absent if the FPZ were a point rather than a finite cohesive zone). But on the nano-scale the lattice is not a continuum and the fracture advances by jumps over the activation energy barriers Q on the surface of the state potential Π (free energy) of the lattice block. These barriers cause that the diagram $P(u)$ is wavy, as shown in Fig. 2b, where the radial lines marked a_1, a_2,... correspond to unloading lines for subsequent crack lengths ending at different atomic pairs marked in Fig. 1a. The interatomic crack propagates by jumps from one crack length to another (Fig. 2b, c). During each jump, one barrier on the potential Π as a function of u must be overcome (see the wavy potential profile in Fig. 2c). After each jump, at each new crack length, there is a small decrease $\Delta\Pi$ (Fig. 2c,d) of the overall potential Π of the atomic lattice block, corresponding to a small advance along the load-deflection curve $P(u)$ (Fig. 2a,b). During each jump, the separation of opposite atoms (in their equilibrium positions) increases by only a small fraction of their initial distance h_a.

Due to thermal activation, the states of the atomic lattice block fluctuate and can jump over the activation energy barrier in either direction (right or left in Fig. 2b, c, d), though not with the same frequency f. Let Q_0 be the activation energy barrier if there is no change of crack length. When the cohesive crack length (defined by the location of state 3 in Fig. 1c) jumps by one atomic spacing, h_a (i.e, from a_i to a_{i+1}, i = 1,2,3,...), the activation energy barrier is changed by a small amount ΔQ corresponding to the energy release by fracture (Fig. 2c,d) associated with the equilibrium load drop ΔP caused by fracture (Fig. 2a).

Now note that $[\partial\Pi(P,a)/\partial a]_P/b = \mathcal{G}$ = energy release rate = $(P^2/2b)\,\mathrm{d}C(a)/\mathrm{d}a$, where b = length of crack front in the third dimension (width) and $C(a)$ = elastic compliance (Fig. 2b) of the atomic lattice block as a function of the crack length a. Further note that $\mathcal{G} = D_a\, g(\alpha)\sigma^2/E$ where E = elastic Young's modulus for the continuum approximation of the lattice, D_a = total length (or dimension) of the cross section of the lattice (Fig. 1a), σ = remote average stress (Fig. 1a) applied on the lattice (which is proportional to P/bD_a), $g(\alpha)$ is the dimensionless energy release rate function of linear elastic fracture mechanics of continuous bodies, characterizing the fracture and block geometry [13], and $\alpha = a/D_a$. Accordingly, we may write:

$$\Delta Q = h_a\left[\frac{\partial \Pi(P,a)}{\partial a}\right]_P = h_a b \mathcal{G} = h_a b D_a g(\alpha)\sigma^2 / E = \sigma^2 V_a / E \tag{1}$$

where $V_a = V_a(\alpha) = h_a b D_a g(\alpha)$ = activation volume of the lattice crack (if the applied stress tensor is written as $\sigma \boldsymbol{s}$ where σ = stress parameter, one could more specifically write $V_a = \boldsymbol{s} : \boldsymbol{v_a}$ where $\boldsymbol{v_a}$ = activation volume tensor, as in atomistic theories of phase transformations in crystals [2]).

Since the crack jump by one atomic spacing h_a is very small, the activation energy barrier for a forward jump, $Q_0 - \Delta Q/2$, differs very little from the activation energy barrier for a backward jump, $Q_0 + \Delta Q/2$. So the jumps of the state of the atomic lattice block, characterized by its free energy potential Π, must be happening in both forward and backward directions, although at different rates. According to the transition-rate theory [23, 26], in the limit of a large free-energy barrier, $Q_0 >> kT$, the first-passage time for each transition is given by Kramers' formula [28], and the difference in the frequencies of the forward and backward jumps, or the net frequency of crack length jumps, is

$$f_b \sim \nu\left(e^{-[Q_0-\sigma^2 V_a/2E]/kT} - e^{-[Q_0+\sigma^2 V_a/2E]/kT}\right) = 2\nu e^{-Q_0/kT}\sinh\frac{\sigma^2 V_a}{2EkT} \sim C_f\sigma^2 \tag{2}$$

where $C_f = \dfrac{\nu\sigma^2 V_a}{EkT}e^{-Q_0/kT}$, T = absolute temperature, k = Boltzmann constant, V_a corresponds to some effective critical value of α, and ν is a characteristic attempt frequency for the reversible transition (e.g. kT/h, where h = Planck's constant, which can be set by a shift of the activation free energy). The last expression is an approximation for small stress σ, which is justified by the fact that for large structures only the left far-out tail of cdf of strength matters [11, 12]. More specifically, we require $\Delta Q << kT << Q_0$ or $\sigma << \sqrt{EkT/V_a}$.

Note the difference from the macro-scale continuum fracture, where the jumps representing fracture reversal play no role because the crack face separations of interest equal very many atomic spacings, rather than a small fraction of one atomic spacing. Also note that, for fracture on the macro-scale, ΔQ is entirely negligible and the free energy change is smooth (as shown by the smooth curve in Fig. 2c).

The net frequency f_b, which is proportional to failure probability, was in previous simplified analysis [11, 12] shown to depend linearly on stress σ on the atomic scale, i.e., to follow a power law of exponent 1, while in Eq. 2 we got a power law of exponent 2. It that a conflict?

No, because it was also shown that the passage to a higher scale, which involves a parallel coupling, raises the exponent of the power-law tail of the cdf of strength. The previous simpler argument dealt with the potential of individual atoms while the present refined and more specific argument deals with a block of many atoms. This transition involves solution of an elasticity problem with a crack, in which the compatibility conditions of the strain field play the role of parallel coupling constraints. So, an increase of exponent must be expected.

Size Effect on Strength Distribution

The foregoing analysis implies that the far-left tail of strength cdf at nanoscale must be a power law. It has been demonstrated that the cdf of strength of quasibrittle structures of positive geometry [5] (i.e. structures that fail at crack initiation) can be modeled as a chain of finite-size RVEs, and a single RVE can be statistically represented by a hierarchical model consisting of bundles of only 2 long sub-chains, each of them consisting of sub-bundles of 2 or 3 long sub-sub-chains of sub-sub-sub bundles, etc. till the nano-scale lattice is reached [11, 12].

As an example of the hierarchy of scales, one could mention concrete, a quasibrittle silicate material totally disordered from the nano-scale. The lowest scale, of the order of 10^{-9} m, consists

mainly of crystalline platelets and needles of calcium silicate hydrates (C-S-H) with the dimension of perhaps 10 atoms. There is no larger crystalline structure. The next scale, of the order of 10^{-8} m consists of packed C-S-H globules. The next, of the order of 10^{-7} to 10^{-6} m, consists of mainly nano-porous cement gel (or tobermorite gel). The next, of the order of 10^{-5} to 10^{-4} m, represents the cement gel, containing capillary voids (>10^{-6} m), CaO crystals, etc. The next, of the order of 10^{-3} to 10^{-2} mm, represents the cement mortar. Lastly, on the scale of >10^{-1} m, one has concrete.

For both ductile and brittle responses, it is shown that the parallel coupling raises the power-law tail exponent in an additive manner and drastically shortens the reach of the power-law tail, while the series coupling preserves the power-law exponent while extending the reach of the power-law or Weibull tail [11, 12]. The consequence of hierarchical model is that the cdf of RVE strength must have a very broad Gaussian core, onto which a power-law tail of an exponent equal to the Weibull modulus is grafted at the failure probability of about 10^{-3} to 10^{-4}. As the structure size increases (or the number of equivalent RVEs increases), the grafting point moves to a higher probability. Eventually, for sufficiently large structures, the entire strength distribution becomes Weibullian.

Fig. 3 shows the optimum fits for the existing experimental histograms of strength of industrial and dental ceramics by the present theory. As commonly observed for other quasibrittle materials such as cement mortar and concrete, there is a kink in the strength histograms, which cannot be explained by the Weibull theory with zero threshold and was thought to require the use of a finite threshold. The excellent fits by the present theory show that finite threshold is not necessary, and that the kink is a natural consequence of the quasibrittleness of the structure, following from the fact that Eq. 2 contains a hyperbolic sine rather than an exponential of stress square. The resulting mean stochastic response of nominal strength agrees with the tests of mean size effect and with the predictions by other established mechanical models such as the cohesive crack model [5, 13], crack band model [13] and nonlocal damage model [8]. The size effect law for nominal strength of structures can be expressed via asymptotic matching as [5, 6]:

$$\bar{\sigma}_N = \left[\frac{N_a}{N} + \left(\frac{N_b}{N} \right)^{s/m} \right]^{1/s} \tag{3}$$

in which N is the equivalent number of RVEs represented by the number of elements in the weakest-link model of the structure, and N_a, N_b, m, s are constants to be found from four asymptotic matching conditions. It is shown that the m-value must be the same as the Weibull modulus of the material, coinciding with the exponent of the power-law tail of strength cdf of one RVE. To obtain the remaining three parameters, one may solve three simultaneous equations expressing three asymptotic matching conditions [9]: $[\bar{\sigma}_N]_{N\to 1}$, $[\mathrm{d}\bar{\sigma}_N / \mathrm{d}N]_{N\to 1}$, and $[\bar{\sigma}_N N^{1/m}]_{N\to\infty}$.

Necessity of Zero Threshold

The experimentally observed deviations of the strength histograms of coarse-grained ceramics from the two-parameter Weibull distribution have recently led to a wide-spread adoption of the three-parameter Weibull distribution, which has a finite threshold. However, the misfit of the experimental histogram has been remedied only partly. Using the three-parameter Weibull model to fit the well-known Weibull's strength histograms which include thousands of data [30], a systematic deviation from the experimental histogram still remains at the high probability end while the present theory gives much better fits (Fig. 4) [11, 12]. Therefore, one may conclude that the overall experimental evidence, as it now exists, does not support the argument for nonzero threshold.

The distinction between three-parameter Weibull distribution and the present theory becomes much clearer by considering the size effect on mean nominal strength of structure. If the probability

density function (pdf) of strength or cdf of one RVE are known, i.e. $p_1(\sigma_N)$ and $P_1(\sigma_N)$, the mean strength of structure having the size of N_{eq} equivalent RVEs can be calculated as:

$$\bar{\sigma}_N = \int_0^\infty \sigma_N N_{eq}[1-P_1(\sigma_N)]^{N_{eq}-1} p_1(\sigma_N)\mathrm{d}\sigma_N \tag{4}$$

With the present theory, the resulting size effect curve for the mean strength according to Eq. 4 matches the type I energetic-statistical size effect law shown in Eq. 3 [5, 6, 11, 12]. For comparison, one can calculate the mean size effect curve when the three-parameter Weibull model is extrapolated from size D_0 (corresponding to N_0) to size D (corresponding to N):

$$\bar{\sigma}_N = \int_0^\infty \left[1-\left\langle \frac{\sigma_N-\sigma_0}{s_0}\right\rangle^m\right]^{N/N_0} \mathrm{d}\sigma_N = \sigma_0 + s_0\Gamma\left(1+\frac{1}{m}\right)\left(\frac{N_0}{N}\right)^{1/m} \tag{5}$$

It is clear that Eq. 5 deviates from Eq. 3 for large size structures. For sufficiently large structures, the mean size effect curve depicted by Eq. 3 converges to the power-law size effect of the two-parameter Weibull model, while the mean size effect curve extrapolating the three-parameter Weibull model has a diminishing slope (in log-log scale) and for large-size structures asymptotically approaches the threshold strength σ_0. These features of the mean size effect curve for non-zero threshold contradict the predictions of other mechanical models such as the crack band model and non-local model, and also the existing experimental observations [15]. This invalidates the argument for a non-zero threshold.

Generalization to Lifetime at Given Stress

The time rate $\dot{a} = \mathrm{d}a/\mathrm{d}t$ of static crack propagation through the atomic lattice can reasonably be assumed to be proportional to the frequency of jumps over the activation energy barriers (Fig. 1b) on the surface of the free energy potential Π of the atomic lattice block, as given by Eq. 2; i.e.

$$\frac{\mathrm{d}a}{\mathrm{d}t} = v_a\left(2e^{-Q_0/kT}\sinh\frac{V_0 g(\alpha)\sigma^2}{EkT}\right) \tag{6}$$

or

$$\frac{\mathrm{d}a}{\mathrm{d}t} \approx v_a e^{-Q_0/kT} g(\alpha)\frac{\sigma^2}{\eta_T^2} \tag{7}$$

where $V_0 = bhD_a = V_a(\alpha)/g(\alpha)$, $\eta_T = (EkT/2V_0)^{1/2}$. Here t = time, v_a is a parameter of the dimension of velocity, which could depend on α but probably can be considered as constant; η_T is a temperature dependent parameter of the dimension of stress; and V_0 is a constant with the meaning of the activation volume for unit energy release rate. The last approximation in Eq. 7 is valid for small σ, i.e., for the left tail of the distribution of σ. Noting that the stress intensity factor $K(\alpha) = \sigma[D_a g(\alpha)]^{1/2}$, one may rewrite this approximation as:

$$\frac{\mathrm{d}a}{\mathrm{d}t} \approx v_a e^{-Q_0/kT}\frac{K^2}{\eta_T^2 D_a} \quad \textbf{(for small } K\textbf{)} \tag{8}$$

Eq. 6 can be integrated by parts from $t = 0$ to $t = \tau$ = lifetime, which gives the following condition for attaining lifetime τ:

$$D_a \int_{\alpha_0}^{\alpha_{cr}} \frac{\mathrm{d}\alpha}{\sinh(V_0 g(\alpha)\sigma^2 / EkT)} = 2v_a e^{-Q_0/kT}\tau \tag{9}$$

Here α_0, α_{cr} are the initial and the critical values of relative crack length $\alpha = a/D_a$. For small σ, upon integrating by parts Eq. 7, one gets for the attainment of lifetime the condition:

$$e^{-Q_0/kT}\frac{\sigma^2}{\eta_T^2}\tau = C \tag{10}$$

where $C = \dfrac{D_a}{v_a}\displaystyle\int_{\alpha_0}^{\alpha_{cr}} \frac{\mathrm{d}\alpha}{g(\alpha)}$

Now it should be noted that Eq. 8 has the form of Evans' law [20, 29]:

$$\dot{a} = c_1 K^n e^{-Q_0/kT} \tag{11}$$

which may be equivalently written as

$$\dot{a} = c_2 \sigma^n [D_a g(\alpha)]^{n/2} e^{-Q_0/kT} \tag{12}$$

where c_1 and c_2 are constants. Exponent n, however, is here equal to 2, while from the testing of various ceramics it is known that n is typically larger than 10 [25]. Why this discrepancy?

The explanation, which is a key idea, is that the empirical large value of n applies only on the macro-scale (or the material scale on an RVE), while the value of $n = 2$ applies on the nano-scale of atomic lattice block. For small σ at the tail of strength distribution, these two widely separated scales may be related by a model with a hierarchy of series and parallel couplings, the same as introduced earlier for strength statistics [11, 12]. This model shows that the parallel couplings in the model raise the exponents of the distribution tails of not only σ but also τ. Eq. 10 applies on the scale of the atomic lattice block, and the hierarchical model indicates that, for transition to the macro-scale of an RVE, the exponent must be raised as follows:

$$\psi(\sigma,\tau) = e^{-Q_0/kT}\frac{\sigma^{np}}{\eta_T^{np}}\tau^r = C \tag{13}$$

where exponent r is an empirical constant ($r > 1$).

Eq. 13 can be regarded as either the critical condition for failure stress σ at given lifetime τ, or as the critical condition for lifetime τ at given stress σ. The inequality $\psi(\sigma,\tau) > C$ means that the structure is failing, and $\psi(\sigma,\tau) < C$ means that it is surviving. The fact that the same equation (Eq. 15) must characterize both the strength limit σ and the lifetime limit τ is clarified by Fig. 5 (right), where the dashed curves represent the response for rapid loading after the stress σ has been held constant for various lengths of time. With increasing duration of constant stress, the stress peaks in the subsequent rapid loading are getting lower (which has been documented experimentally for concrete). When this duration approaches the lifetime τ, the stress peak converges to the long-time stress value σ.

Now, what is the failure probability, P_f? Since, in a quasi-steady state, the failure probability on the macro-scale (or RVE scale) is proportional to the frequency of breaking the critical condition for lifetime given by Eq. 13, we conclude that the cdf of lifetime may be written as follows:

$$P_1 = \min\left(e^{-Q_0/kT} \frac{\sigma^2}{\eta_T^2} \tau, 1 \right) \quad \text{(for atomic lattice scale)} \tag{14}$$

where the "min" and "1" need to be introduced to achieve normalization of cdf. The function $g(\alpha)$ has been dropped from these equations since it should be evaluated for a certain effective (or average, critical) value α_{cr} of relative length of the atomic lattice crack, and thus is a constant.

In analogy to the strength statistics of bundles and chains (or parallel and series couplings), it appears from numerical simulations that the exponent of the power-law tail for cdf of lifetime is preserved by a series coupling and is increased by parallel coupling, for both brittle and ductile behaviors [27], whereas the probability reach of the power-law tail of lifetime cdf is drastically shortened by parallel coupling and drastically extended by series coupling. Because parallel couplings generally produce a Gaussian distribution, regardless of the distributions of the coupled elements [19], it further follows that the rest of lifetime cdf beyond the tail (i.e., its core and far-right tail), must have the Gaussian (or normal) distribution, with a relatively sharp transition. Similar to strength cdf, this transition of lifetime cdf can be simplified as a point transition at a grafting point of the power-law tail and Gaussian core.

For the strength statistics of bundles and chains (or parallel and series couplings), there exists an analytical proof [12] (based on Daniel's [19] recursive equation for the cdf of fiber bundles) that the exponent of the power-law tail for cdf of strength is preserved by a series coupling and is additive for parallel coupling, for both brittle and ductile behaviors, whereas the reach of the power-law tail of lifetime cdf is drastically shortened by parallel coupling and drastically extended by series coupling. Because parallel couplings generally produce a Gaussian distribution, regardless of the distributions of the coupled elements [19], it further transpires that the rest of strength cdf (beyond the tail, i.e., the core and the far-right tail), must have the Gaussian (or normal) distribution, with a relatively sharp transition, and that this transition of strength cdf can be simplified as a point transition at a grafting point of the power-law tail and Gaussian core. Therefore, in Eq. 14, we will raise σ^2 to exponent $p > 1$ (whose meaning is the minimum of the sum of strength powers among all possible cuts separating the model into two halves).

Similar properties of parallel and series couplings appear to hold true for the cdf of lifetime. Although an analytical proof for parallel coupling of ductile or brittle elements has not yet been obtained, the power-law tail appears to be always preserved, and the same hierarchical model (Fig. 5 left) appears to apply (for a special rule of load sharing in a fiber bundle, the exponent of a power-law tail of lifetime cdf has been proven to be additive [27]).

It might be thought that exponent r should be equal to p. However, experiments on ceramics and fiber composites reveal that r is much smaller than p and should be equal to about 2. This means that the number of cuts necessary to separate the hierarchical model in Fig. 5 is lower for long-time loading than it is for short-time loading. A plausible explanation is that some of the links in the hierarchical model fail with the passage of time before the lifetime is reached. Physically, the delayed failure of these links may be explained as gradual time-dependent development of microcracks within a loaded representative volume. Only the links remaining at the end of lifetime decide the strength (this further suggests that exponent r might better be considered as time dependent, but there are no data justify such a complication).

Since the tail of lifetime cdf is raised to a power r lower than p, Eq. 14 may be extended from the atomic lattice block scale to the RVE scale as follows:

$$P_f = \min\left(e^{-Q_0/kT} \frac{\sigma^{np}}{\eta_T^{np}} \tau^r, 1 \right) \text{ (for RVE scale)} \tag{15}$$

It must be emphasized that the cdf expressions in Eqs. 14 and 15 are valid only for the far-left tails of cdf. Based on the common precision in the experimental observations of the deviations from Weibull statistics (or from perfectly brittle behavior), the validity of these cdf expressions extends (for what is understood as quasibrittle materials) to the failure probability of about 0.0001 to 0.01. For ductile materials, the reach of the power-law tail is much shorter, and for brittle materials it is longer.

Fig. 6 shows that the present theory fits the existing lifetime histograms of organic fiber (Kelvar 49) composites quite well [18]. These histograms are plotted in the Weibull scale, in which the Weibull cdf is a straight line of slope r and the Gaussian cdf is a curve deviating to the right. For the size effect on lifetime distribution, the cdf of lifetime for small-size structures is again depicted as Gaussian except for the far-left tail. For sufficiently large structures, the lifetime distribution approaches the Weibull distribution with a modulus equal to r.

Knowing the size effect on lifetime cdf, one can compute the size effect on the mean lifetime, which can be approximately deduced by a matching technique similar to that leading to Eq. 3:

$$\bar{\tau} = \left[\frac{K_a}{N} + \left(\frac{K_b}{N} \right)^{q/r} \right]^{1/q} \tag{16}$$

The four constants in this equation, K_a, K_b, q, r, can be determined from asymptotic conditions. Experimental evidence indicates that the Weibull modulus r for lifetime distribution is very low compared to that for strength distribution [18, 21, 25]. Therefore, the size effect on the mean lifetime is much stronger than the size effect on the mean nominal strength of the structure.

Atomistic Derivation of Paris Law

The Paris (or Paris-Erdogan) law for crack growth due to cyclic loading reads

$$\Delta a/\Delta N = C_p(\Delta K)^n \tag{17}$$

where C_P = empirical constant, N is the number of cycles and ΔK is the amplitude of the stress intensity factor, and n (>1) is an empirical exponent. Evidently, this law is analogous to Evans' law (Eq. 11) for crack growth rate under constant load. Similarly as that equation, the Paris law can be expressed in terms of the stress amplitude

$$\Delta s = \Delta K/[D_a\, g(\alpha)]^{1/2} \tag{18}$$

which can be derived from the statistics of the atomistic lattice crack growth in a similar manner. The only difference is that now the stress amplitude Δs must be interpreted as the amplitude of the shakedown stress in the microstructure [22] rather than the amplitude of the applied stress σ. Of course, this derivation rests on certain simplifying assumptions, which explains why deviations from Paris law exist on a broader scale of observations [4, 16, 13].

Closing Remarks

For a long time, the statistics of brittle failures has been based on the statistics of small flaws. This has not been quite satisfactory for various reasons, e.g. because fracture of concrete is very similar

to fracture of ceramics, yet the definition of a flaw in concrete, a totally disordered material, is subjective and ambiguous. It now transpires that a more fundamental basis of the statistics of brittleness lies in thermally activated bond breaking within the atomic structure on the nano-level.

The theory sketched here (which will be expounded in detail in a forthcoming journal article) appears to fit all the existing experimental data on the strength and lifetime histograms, on the size effect (in specimens of positive geometry), and on the crack growth rate. The aim has been to provide a logical, consistent and comprehensive explanation to the existing data. The present derivations involve many simplifications and hypotheses, and so they should not be misinterpreted as a deductive proof. What justifies these simplifications is the achievement of comprehensive agreement with test results.

Nevertheless, there are a few features that appear to be a necessary consequence of the atomistic basis — for instance the vanishing of the strength threshold, which is a feature independent of the particular simplifications made and is common to various alternative versions of the present theory.

The nano-mechanical explanation of test results presented here also seems to provide a springboard to further advances, for instance in the theory of material fatigue.

Acknowledgement: Various parts of the present research were financially supported by the U.S. National Science Foundation under grant CMS-0556323 to Northwestern University, by Boeing, Inc., under grant N007613 to Northwestern University, and by the U.S. Department of Transportation through the Infrastructure Technology Institute of Northwestern University under grant 0740-357-A222. Thanks for incisive and stimulating comments are due to Prof. Gregory Barenblatt of the University of California, Berkeley.

References

[1] Abraham, F. F., Broughton, J. Q., Bernstein, N. and Kaxiras, E., "Spanning the continuum to quantum length scales in a dynamical simulation of brittle fracture," Europhys. Lett. 44 (6), 1998, 783-787.

[2] Aziz, M. J., Sabin, P. C., and Lu, G. Q., "The activation strain tensor: Nonhydrostatic stress effects on crystal growth kinetics," Phys. Rev. B 41, 1991, 9812-9816.

[3] Barenblatt, G.I. "The formation of equilibrium cracks during brittle fracture. General ideas and hypothesis, axially symmetric cracks." Prikl. Mat. Mekh. 23, 1959, 434-444.

[4] Barenblatt, G.I. "Scaling phenomena in fatigue and fracture." Int. J. Frac. 138, No. 1-4, 2006, 19-35.

[5] Bažant, Z. P. "Scaling theory of quaisbrittle structural failure". Proc. of National Academy of Sciences 101 (37), 2004, 13397-13399.

[6] Bažant, Z. P. Scaling of Structural Strength, 2nd Ed., Elsevier, London 2005.

[7] Bažant, Z. P. and Jirásek, M. "R-curve modeling of rate and size effects in quasibrittle fracture." Int. J. of Frac. 62, 1993, 355-373.

[8] Bažant, Z. P. and Jirásek, M. "Nonlocal integral formulations of plasticity and damage: Survey of progress." J. Engrg Mech., ASCE, 128(11), 2002, 1119-1149.

[9] Bažant, Z. P. and Le, J.-L. "Atomistically based prediction of size effect on strength and lifetime of composites and other quasibrittle materials". Proc. of 49th AIAA/ASME/ASCE/AHS/ASC Structure, Structural Dynamics, and Materials Conference, Schaumburg, Illinois, 2008.

[10] Bažant, Z.P., and Pang, S.-D. "Revision of Reliability Concepts for Quasibrittle Structures and Size Effect on Probability Distribution of Structural Strength." Safety and Reliability of Engrg. Systems and Structures (Proc., 8th Int. Conf. on Structural Safety and Reliability, ICOSSAR 2005, held in Rome), G. Augusti, G.I. Schueller and M. Ciampoli, eds., Millpress, Rotterdam 2005, pp. 377-386.

[11] Bažant, Z. P. and Pang, S.-D. "Mechanics based statistics of failure risk of quasibrittle structures and size effect on safety factors". Proc. National Academy of Sciences 103 (25), 2006, 9434-9439.

[12] Bažant, Z. P. and Pang, S.-D. "Activation energy based extreme value statistics and size effect in brittle and quasibrittle fracture". J. of the Mechanics and Physics of Solids 55, 2007, 91-134.

[13] Bažant, Z. P. and Planas, J. Fracture and Size Effect in Concrete and Other Quasibrittle Materials, CRC Press, 1998.

[14] Bažant, Z. P. and Prat, P. C. "Effect of temperature and humidity on fracture energy of concrete." ACI Mater. J. 85-M32, 1988, 262-271.

[15] Bažant, Z. P., Vořechovský, M., and Novák, D. "Asymptotic prediction of energetic-statistical size effect from deterministic finite element solutions." J. Engrg. Mech, ASCE, 128, 2007, 153-162.

[16] Bažant, Z. P. and Xu, K. "Size effect in fatigue fracture of concrete." ACI Materials J. 88(4), 1991, 390-399.

[17] Broughton, J. Q., Abraham, F. F., Bernstein, N. and Kaxiras, E., "Concurrent coupling of length scales: Methodology and Application," Phys. Rev. B 60, 1999, 2391-2403.

[18] Chiao, C. C., Sherry, R. J., and Hetherington, N. W. "Experimental verification of an accelerated test for predicting the lifetime of organic fiber composite." J. Comp. Mater. 11, 1977, 79-91.

[19] Daniel, H. E. "The statistical theory of the strength of bundles and threads." Proc. R. Soc. London A, 183, 1945, 405-435.

[20] Evans, A. G. and Fu Y. "The mechanical behavior of alumina." In *Fracture in Ceramic Materials*, Noyes Publications, Park Ridge, NJ, 1984, 56-88.

[21] Fett, T., and Munz, D. "Static and cyclic fatigue of ceramic materials." In Ceramics Today – Tomorrow's Ceramics", Elsevier Publisher, BV, 1991, 1827-1835.

[22] Jirásek, M. and Bažant, Z. P. Inelastic Analysis of Structures, J. Wiley & Sons, London and New York.

[23] Kaxiras, E. *Atomic and Electronic Structure of Solids* (Cambridge University Press, 2003).

[24] Marder, M. "Effect of atoms on brittle fracture," Int. J. of Frac. 130**,** 2004**,** 517-555.

[25] Munz, D., and Fett, T. Ceramics Mechanical Properties, Failure Behaviour, Materials Selection. Springer, 1999.

[26] Phillips, R. *Crystals, Defects and Microstructures: Modeling Across Scales* (Cambridge University Press, 2001).

[27] Phoenix, S. L., and Tierney, L.-J. “A statistical model for the time dependent failure of unidirectional composite materials under local elastic loading-sharing among fibers.” Engrg. Frac. Mech. 18 (1), 1983, 193-215.

[28] Risken, H. *The Fokker-Planck Equation*, second edition (Springer Verlag, 1989).

[29] Thouless, M. D., Hsueh, C. H., and Evans, A. G. “A damage model of creep crack growth in polycrystals.” Acta Metall. 31 (10), 1983, 1675-1687.

[30] Weibull, W. “The phenomenon of rupture in solids.” Proc. Royal Swedish Inst. Eng. Res. 153, Stockholm, 1939, 1-55.

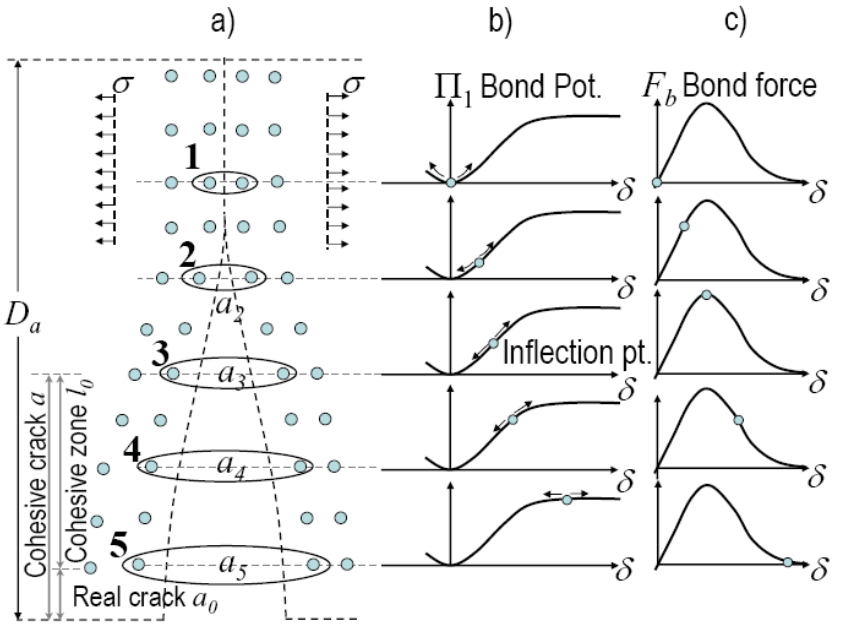

Fig. 1 Fracture of atomic lattice

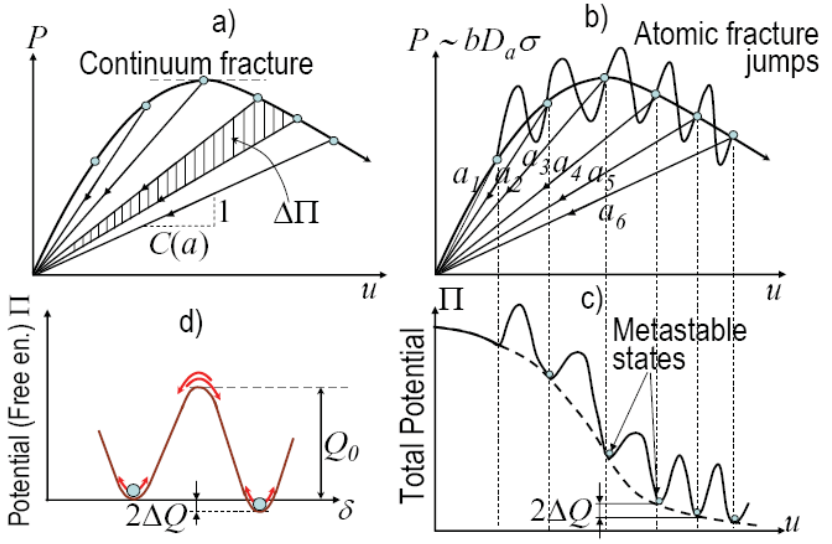

Fig. 2 Load displacement curve of atomic lattice block

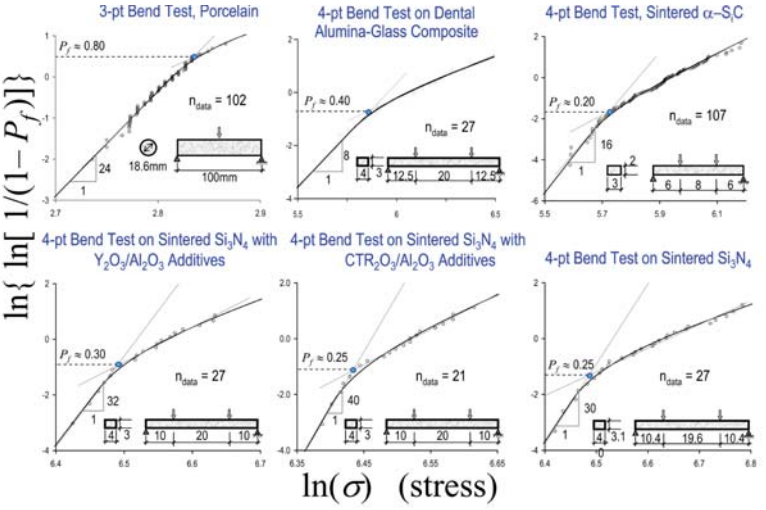

Fig. 3 Optimum fits for strength histograms for industrial and dental ceramics

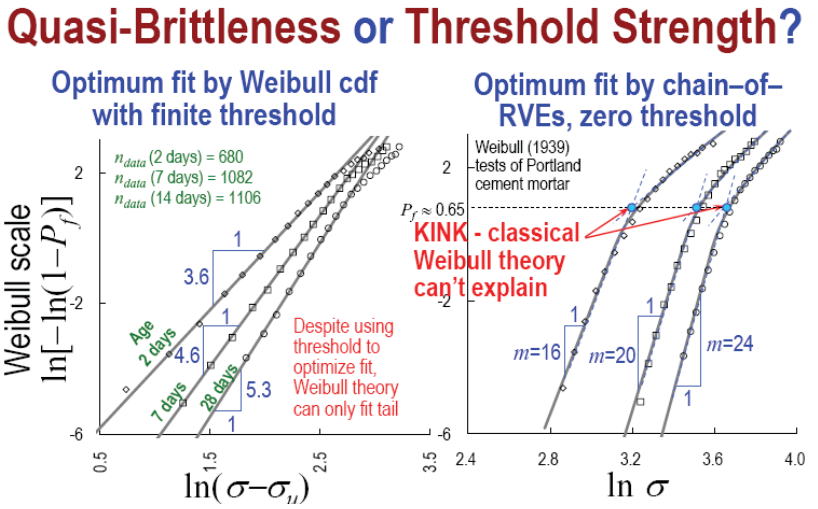

Fig. 4 Optimum fits for Weibull's histograms [30] by three-parameter Weibull model (left)and present theory (right)

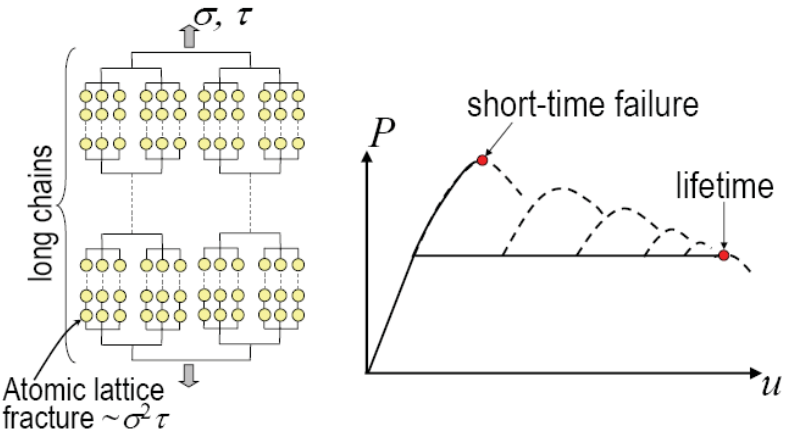

Fig. 5 Hierarchical series-parallel model for an RVE (left) and its load-deflection behavior (right)

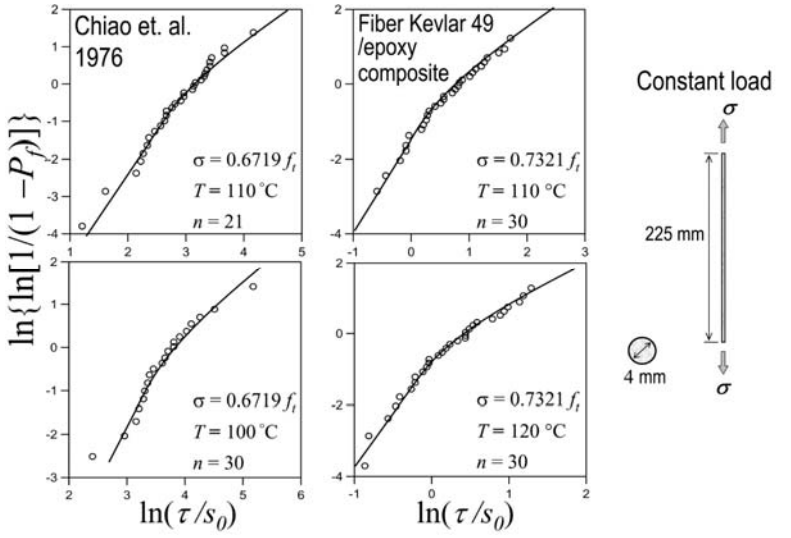

Fig. 6 Optimum fits for lifetime histograms for organic fiber composites [18]